



A new genus and species of ilyophine eel (Anguilliformes: Synphobranchidae: Ilyophinae) from the Arabian Sea, western Indian Ocean

KENNETH A. TIGHE^{1,3} & PARAMASIVAM KODEESWARAN²

¹Department of Vertebrate Zoology, National Museum of Natural History, Smithsonian Institution, Washington, DC, USA.

 tighek@si.edu;  <https://orcid.org/0000-0003-1127-0949>

²Centre for Marine Living Resources and Ecology, Ministry of Earth Sciences, Government of India, Kochi—682 508, Ernakulam, Kerala, India.

 kodyvenkat1995@gmail.com;  <https://orcid.org/0000-0002-4636-3056>

³Corresponding author

Abstract

A new genus and species of ilyophine eel, *Branchenchelys megacephala*, is described based on five specimens collected in the Arabian Sea, western Indian Ocean. The new genus is distinguished from all other ilyophine genera by its relatively large head with large gill openings and a very large branchial chamber with an increased number of branchiostegal rays and hypertrophied gill filaments.

Key words: Pisces, Teleostei, taxonomy, *Branchenchelys megacephala*

Introduction

The subfamily Ilyophinae (family Synphobranchidae) presently consists of six genera and ca. 41 species (Fricke *et al.*, 2025) and is the most speciose and morphologically diverse of the synphobranchid subfamilies. The number of species in the subfamily is likely to increase, as several undescribed species are currently under study by the authors and others. Among these undescribed species are five specimens collected in the Arabian Sea, western Indian Ocean that do not fit into any of the described genera. Two of these specimens were recently cataloged at the Natural History Museum, London, as part of the incorporation of the collection from the Institute of Oceanographic Sciences. The other three specimens were collected from off Karnataka coast, Arabian Sea, southwest coast of India. They are described below as a new genus and a new species.

Materials and methods

General methods for morphometric and meristic data for this study are given in Böhlke (1989). Measurements over 50 mm were made with a 450 mm ruler to the nearest 1 mm, and measurements between 10 and 50 mm were made with a digital caliper to the nearest 0.1 mm. Measurements under 10 mm were taken with an ocular micrometer. All measurements are given as a proportion of the total length (TL) except for subunits of the head, which are presented as proportions of the head length (HL). Vertebral and fin ray counts were taken from radiographs. Total vertebral counts are of all elements, including the hypural plate. Preanal and predorsal vertebral counts were taken using the definitions of Böhlke (1982). Precaudal vertebral counts were taken back to the first vertebra with a clearly posteriorly directed haemal arch. The number of dorsal rays anterior to the anal origin is counted back to a vertical through the first anal ray base. Cyanine blue was used for staining cephalic sensory pores (Saruwatari *et al.*, 1997). Comparative data were taken from Robins & Robins (1976), Robins & Robins (1989) and Ho *et al.* (2015). The osteology of several species in three genera of Ilyophinae (*Attractodenchelys*, *Dysommima*, and *Dysomma*) was described by Robins and Robins (1970). Robins (1971) described the osteology of *Ilyophis brunneus*, and Robins

and Robins (1976) described the osteology of two additional species in the Ilyophinae (*Ilyophis arx* and *Dysomma goslinei*). Description of the osteology of this taxon was based on microCT scans. The holotype and one paratype (BMNH 2016.8.25.789) were scanned on a GE Phoenix v|tome|x M 240/180kV Dual Tube μ CT scanner at the Micro Computed Tomography Imaging Center (mCTIC) at the Smithsonian Institution National Museum of Natural History Scientific Imaging Core Facility (RRID:SCR_025090) with the following settings: 90 kV, 110 μ A, 250 ms exposure time. The resulting x-ray projections were reconstructed into three-dimensional image stacks using the software package datovis reconstruction vers. 2.4.0, and were visualized and segmented using 3D Slicer vers. 5.6.2 (Fedorov *et al.*, 2012). The resulting three-dimensional image stacks were uploaded to MorphoSource (media identification numbers 000769228 and 000769251, respectively). Meristic and morphometric data for the types are presented, with the values of the holotype first, and the values of the paratypes given in brackets. The specimens are deposited at the Natural History Museum, London (BMNH) and the reference collections of Bhavasagara Museum, Centre for Marine Living Resources and Ecology (CMLRE), Cochin, India.

Systematics

Branchenchelys gen. nov.

Type species: *Branchenchelys megacephala* sp. nov.

Diagnosis. A genus of the family Synphobranchidae, subfamily Ilyophinae, defined by its relatively large head with very large branchial chamber supported by numerous branchiostegal rays and with hypertrophied gill filaments and the following combination of characters: large gill openings, with anterior ends close together ventrally, diverging posteriorly and dorsally; possession of enlarged, compound teeth on the vomer and intermaxillary tooth patch; no pectoral fin; lateral line pores restricted to the branchial region of the head; rim of orbital foramen formed totally of ventral extensions of the frontal bone. For other characters, see the description below of *Branchenchelys megacephala*, the type species by designation and monotypy.

Comparative Remarks: *Branchenchelys* can be distinguished from the genera *Ilyophis* and *Meadia* by the presence of compound teeth (versus only simple teeth). *Branchenchelys* can be distinguished from the genus *Atractodenchelys* by the presence of a pair of transversely oriented, enlarged compound teeth on the intermaxillary tooth patch (versus 12 or more simple teeth in an irregular tooth patch). The genera *Dysommia* and *Linkenchelys* have no teeth on the intermaxillary region while *Branchenchelys* has the transverse pair of enlarged compound teeth on the intermaxillary mentioned above. Most members of the genus *Dysomma* have vomerine and intermaxillary dentition similar to *Branchenchelys*. Five species in the genus *Dysomma* (*D. goslinei* Robins & Robins, 1976, *D. longirostrum* Chen & Mok, 2001, *D. melanurum* Chen & Weng, 1967, *D. phuketensis* Prokofiev, 2019, and *D. robinsorum* Ho & Tighe, 2018) have no intermaxillary teeth, while *Branchenchelys* has the transverse pair mentioned above. All other members of the genus *Dysomma* have the combination of a transverse pair of compound teeth on the intermaxillary region and 3–5 compound teeth on the vomerine region of the ethmo-vomer. *Branchenchelys* can be distinguished from most of these species by its relatively large head with enlarged branchial chamber, larger gill openings, and hypertrophied gill filaments. *Dysomma bucephalus* also has a relatively large head, large gill openings, and an enlarged branchial chamber like *Branchenchelys*, but can be distinguished by its nearly complete lateral line (versus lateral line pores restricted to the branchial region of the head in *Branchenchelys*) and presence of a pectoral fin (versus absent in *Branchenchelys*).

Etymology. The generic name *Branchenchelys* is derived from the Greek βράγχια, gills, and εγγελύς, eel, in recognition of the enlarged gill chamber and hypertrophied gill filaments of the type species. The gender is feminine.

Branchenchelys megacephala sp. nov.

Figures 1–14, Table 1

Holotype: BMNH 2016.8.25.788, 195 mm TL, collected off Oman, Arabian Sea, western Indian Ocean, 19° 12' N, 58° 22' E, depth 700–800 m, R.R.S. Discovery Cruise 211, Station 12714#01, Agassiz Trawl, 28 Oct 1994.

Paratypes: BMNH 2016.8.25.789, 148 mm TL, same data as holotype; IO/OV/ANG/00024, 168 mm TL, collected from Mangalore Fishing Harbour, off Karnataka, Arabian Sea, western Indian Ocean, Sanjay Kumar, 10 Jan 2024. IO/SS/ANG/00025, 2 specimens, 155–166 mm TL, collected off Karnataka, Arabian Sea, western Indian Ocean, 13°55' N, 72°38' E, depth 366 m, Sagar Sampada Cruise 404, Epibenthic Dredge, 26 Mar 2024.



FIGURE 1. A: Holotype of *Branchenchelys megacephala*: BMNH 2016.8.25.788, 195 mm TL. B: Paratype of *Branchenchelys megacephala*: BMNH 2016.8.25.789, 148 mm TL.



FIGURE 2. Paratype of *Branchenchelys megacephala* IO/OV/ANG/00024, 168 mm TL. (Photo credit Ravinesh R., CMLRE).

TABLE 1. Morphometrics and meristics of the types of *Branchenchelys megacephala*.

	Holotype	Paratype	Paratype	Paratype	Paratype
	BMNH	BMNH	IO/OV/ANG	IO/SS/ANG	IO/SS/ANG
	2016.8.25.788	2016.8.25.789	00024	00025	00025
Morphometrics					
Total length (mm)	195	138	168	166	155
Proportions (% TL)					
Predorsal length	25.6	24.3	25.4	26.4	26.4
Preal anal length	27.7	27.0	27.8	26.5	28.8
Trunk length	8.8	10.5	6.6	7.0	6.9
Tail length	72.3	73.0	73.2	73.5	71.2
Body depth at gill opening	6.1	6.5	4.9	4.7	6.2
Body width at gill opening	4.4	5.8	2.3	2.2	3.0
Body depth at anus	5.6	5.6	4.2	4.7	4.5
Body width at anus	4.9	4.0	3.4	4.3	4.0
Head depth	7.7	6.6	5.7	6.0	7.2
Head width	4.4	3.8	2.3	2.8	3.0
Head length	18.9	17.2	19.7	19.9	19.8
Proportions (% HL)					
Snout length	13.0	14.1	13.2	13.5	12.6
Eye diameter	4.3	5.4	5.6	4.0	4.1
Postorbital distance	82.7	80.4	79.5	80.2	81.4
Head depth	40.9	38.4	28.7	29.9	36.8
Head width	23.3	22.0	11.8	9.8	15.2
Upper-jaw length	29.3	31.4	30.8	28.4	31.8
Lower-jaw length	27.4	30.6	29.7	27.7	29.7
Interorbital width	10.8	11.0	10.4	8.8	9.8
Gill-opening length	19.0	19.6	24.4	24.5	24.3
Interbranchial width	3.3	3.9	3.4	4.3	4.0
Meristics					
SO pores	3	3	3	3	3
IO (including AD) pores	4	4	4	4	4
POM pores	6 + 1	6 + 1	6 + 1	6 + 1	6 + 1
Branchial pores	5	4	7	7	10
Dorsal rays	231	282	---	---	---
Anal rays	206	238	---	---	---
Anal fin origin at DR	10	15	---	---	---
Predorsal vertebrae	23	23	21	23	23
Preal anal vertebrae	27	28	27	27	28
Precaudal vertebrae	56	56	---	---	---
Total vertebrae	138	134	145	---	---

Diagnosis. As for the genus.

Description. Table 1 gives a summary of meristics and morphometrics for the type series. Total vertebrae 138 (134–145), predorsal vertebrae 23 (21–23), preanal vertebrae 27 (27–28), precaudal vertebrae 56 (56). Dorsal-fin rays 231 (282), anal-fin rays 206 (238), anal origin at dorsal-ray 10 (15). Proportions as percent of TL: predorsal length 25.6 (24.3–26.4), preanal length 27.7 (26.5–28.8), trunk length 8.8 (6.6–10.5), tail length 72.3 (71.2–73.5), depth (at gill opening) 5.5 (2.3–4.9), depth (at anal origin) 5.6 (4.2–6.2), head length (HL) 18.9 (17.2–19.9). Proportions as percent of HL: eye diameter 4.3 (4.0–5.6), interorbital width 10.8 (8.8–11.0), snout length 13.0 (12.6–14.1), upper jaw length 29.3 (28.4–31.8), lower jaw length 27.4 (27.7–30.6), branchial aperture 19.0 (19.6–24.5).

Coloration. Fresh colors. Body brownish, with numerous melanophores; abdomen with almost blue tinge, reaches almost half body length (Fig. 2); head dark pinkish to brown with numerous melanophores in the brachial region. Anus black. Anterior dorsal and anal fin pale, posterior dorsal and anal fin black, caudal fin black. In preservation (Figs. 1–2). Body and head turned dark brown, blue tinged abdomen portion turns pale; posterior dorsal and anal fin black, caudal fin remains black.

Cephalic lateralis pores (Fig. 3B): Head pores minute. Supraorbital pores 3, first pore at ventral end of snout, second pore at snout tip before anterior nostril, third pore slightly larger than both, positioned above and before anterior nostril. Infraorbital pores 4, first pore immediately at base of anterior nostril, second pore between anterior nostril and posterior nostril, third pore behind posterior nostril and under anterior margin of eye, last pore below posterior margin of eye.

Postorbital and supratemporal pores absent. Lateral line 4–10-pores, restricted to the branchial region of the head. Single line of sensory papillae posterior to head, but without open pores.

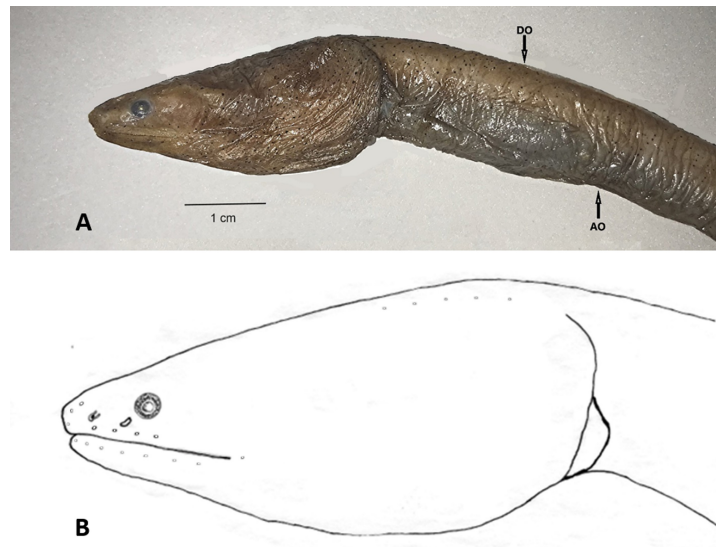


FIGURE 3. A. Head of BMNH 2016.8.25.788. B. Drawing of head of BMNH 2016.8.25.788 showing nostrils and cephalic lateralis pores.

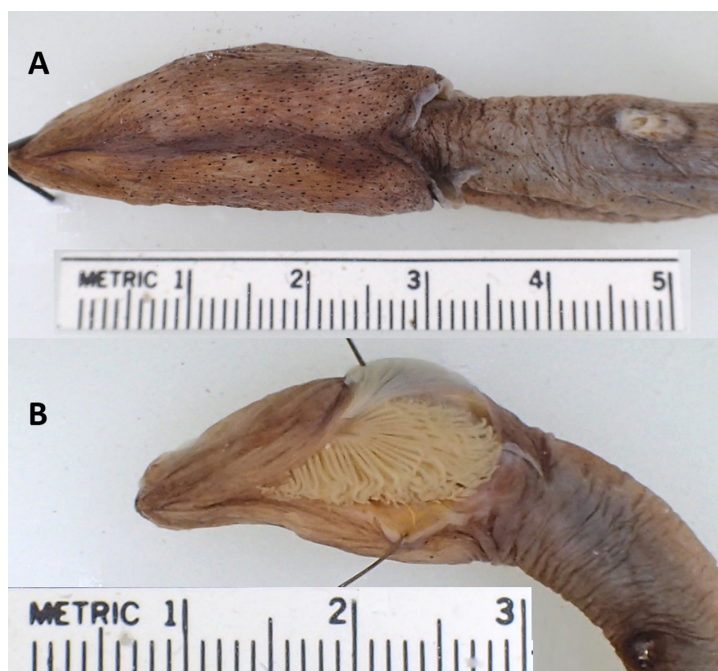


FIGURE 4. A. Ventral surface of anterior of BMNH 2016.8.25.788 showing gill openings. B. Gill chamber of BMNH 2016.8.25.789 showing hypertrophied gill filaments.

Body moderately elongate, very compressed and tapering posterior to anus (Figs. 1–2).

Head large (ca. 1/5 of total length) and relatively deep (Fig. 3). Anterior nostril small and tubular, lateral on snout. Posterior nostril slightly larger, oval, just in front of eye. Gill openings large (ca 1/5 of head length), with anterior ends close together ventrally, diverging posteriorly and dorsally (Fig. 4A); gill filaments hypertrophied (Fig. 4B).

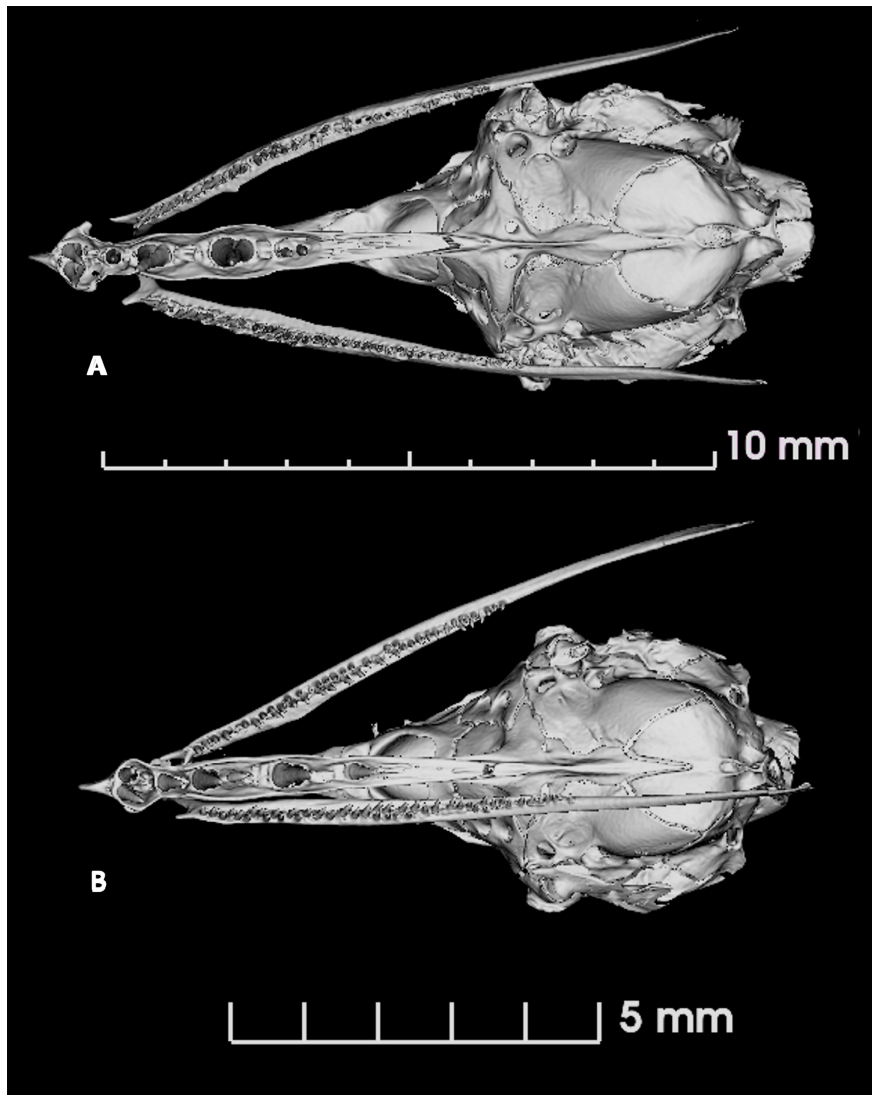


FIGURE 5. MicroCT scan of the skull of *Branchenchelys megacephala*, ventral view showing the vomerine teeth and maxillary teeth. A. BMNH 2016.8.25.788. B. BMNH 2016.8.25.789.

Dentition (Figs. 5–6). There are two transversely oriented compound intermaxillary teeth. Four relatively large, compound vomerine teeth set in epithelial pads, first approximately the same size as intermaxillary teeth, second larger, third largest, and fourth about same size as first. The holotype (Fig. 5A) has 2 small teeth (possibly replacement teeth as they are not fused into a socket) in place of the fourth, while the paratype (Fig. 5B) has a small replacement tooth posterior to the second tooth. The maxillary teeth are conical and slightly recurved, set in a single irregular row of 38–40. There are a few isolated, single teeth set outside of the main row, resulting in a total number of maxillary teeth of 40–45. The dentary teeth (Fig. 6) are set in a single row, teeth decreasing in size gradually from anterior to posterior. The holotype (Fig. 6A) has 33–37 teeth with the anterior 10–12 clearly compound with lateral grooves and figure eight shaped pulp cavities (Fig. 6C–D). The rest of the dentary teeth have round to oval pulp cavities but may be capable of changing into compound teeth, as several of the posterior teeth have small lateral grooves. Also, the paratype (BMNH 2016.8.25.789) is smaller and has fewer anterior compound teeth (ca. 6–7) than the holotype (Fig. 6B). Apparently, some of the teeth can change into compound teeth with growth.

Osteology (Figs. 7–14). The osteology discussed below is based on the two specimens that were microCT scanned. Details of the osteology of *Branchenchelys megacephala* are described individually in the sections below, and differences between *B. megacephala* and the other species will be discussed in the individual sections below.

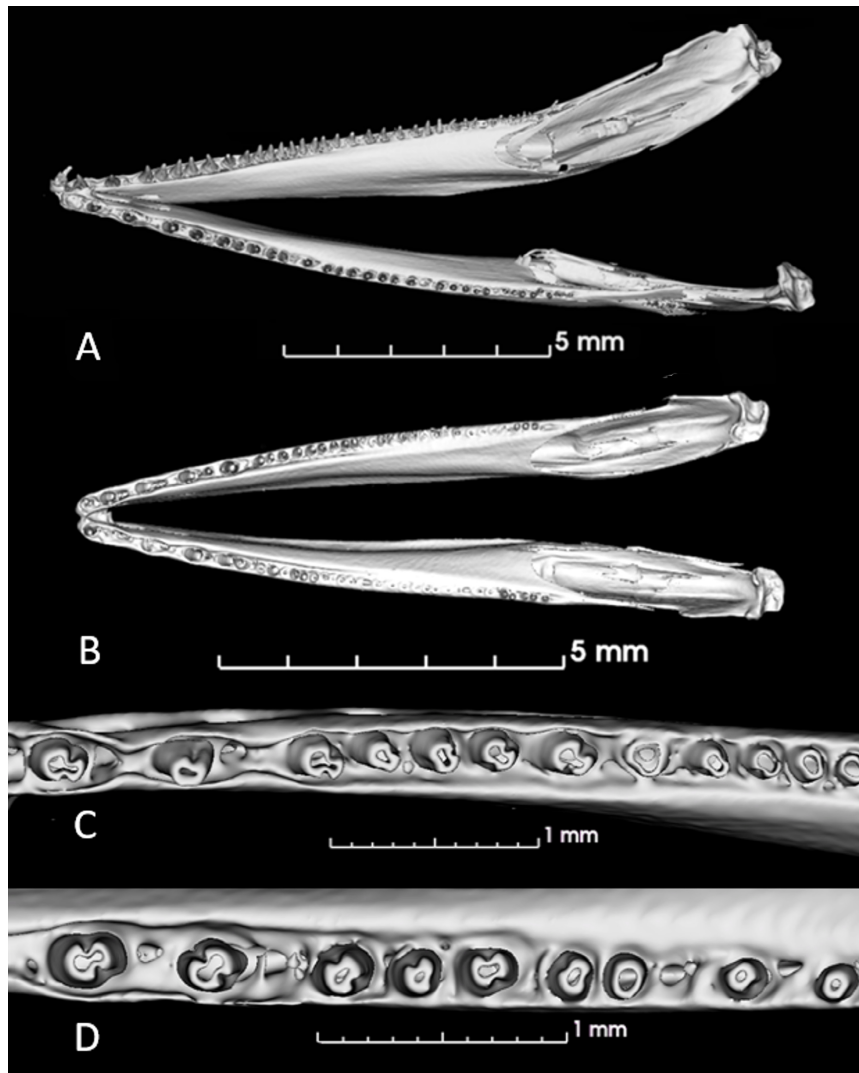


FIGURE 6. MicroCT scan of the mandible of *Branchenchelys megacephala*, ventral view showing mandibular teeth. A. BMNH 2016.8.25.788. B. BMNH 2016.8.25.789. C. Cross-section of anterior teeth of left mandible, BMNH 2016.8.25.788. D. Cross-section of anterior teeth of right mandible, BMNH 2016.8.25.788.



FIGURE 7. Radiograph of BMNH 2016.8.25.788.

Fig. 7 shows the holotype with a radiograph of the entire specimen. Fig. 8 shows a microCT scan of the osteology of the head of the holotype in dorsal, lateral, and ventral views. As can be seen in these radiographs, the skull is relatively short, being ca. 1/3 the length of the head. The gill arches extend from beneath the posterior portion of the skull to a point just over 2/3 of the length of the head. Most of the head consists of the branchial chamber supported by the branchiostegals.

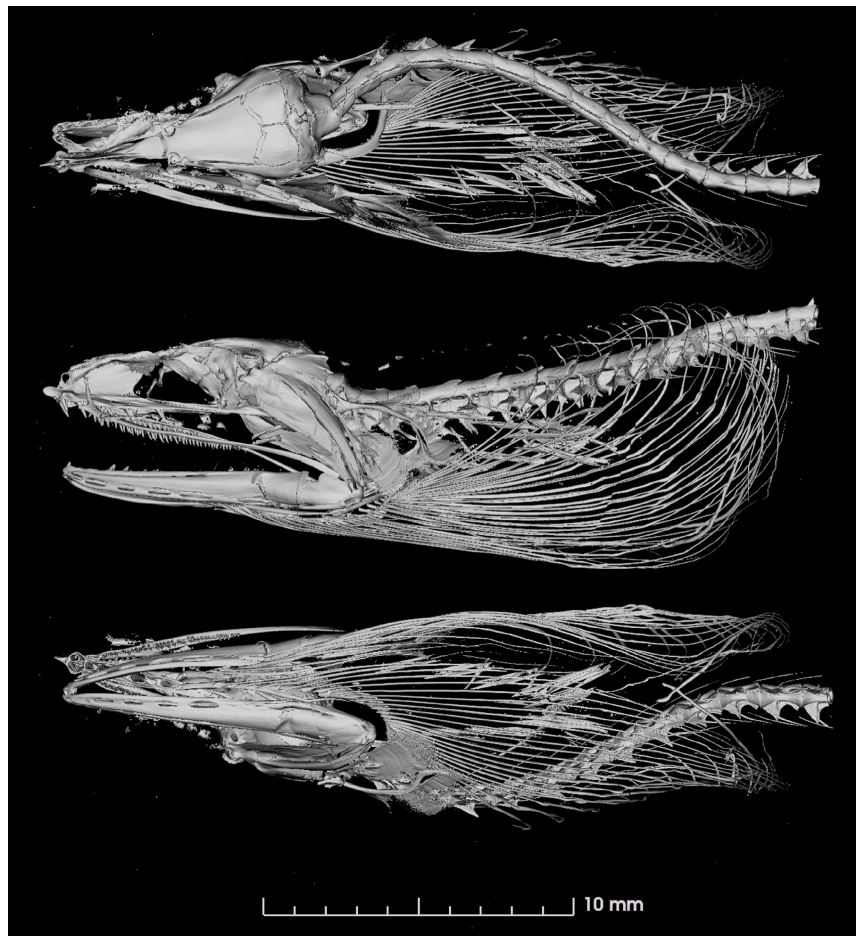


FIGURE 8. MicroCT scan of the anterior portion of holotype of *Branchenchelys megacephala*: BMNH 2016.8.25.788. A. Dorsal view. B. Lateral view. C. Ventral view.

Cephalic lateralis (Fig. 9). The figure shows the cephalic lateralis and lateral line ossicles of the holotype as well as a close-up of the cephalic ossicles of a paratype (BMNH 2016.8.25.789). There are 12 cephalic lateralis ossicles on the dorsal surface of the head, around the eye, and along the upper jaw. The anteriormost on the dorsal surface is the nasal ossicle, which supports the dorsal portion of the nasal chamber. There is no rostral ossicle, and the supraoccipital lateralis pores are anterior to the nasal ossicle. There are two very small ossicles along the portion of the supraorbital canal above the eye and two ossicles on the postocular portion of the infraorbital canal, but there are no pores associated with them. There are six ossicles associated with the infraorbital canal. The relationship of the infraorbital pores with the ossicles could not be determined due to their very small size.

Finally, there is a relatively large, hour-glass shaped ossicle within the orbit and anterior to the eye. This was reported by Robins and Robins (1970) in *Attractodenchelys phrix*, *Dysommima rugosa* and *Dysomma anguillare* although this element was cartilaginous in the latter two species. They considered this element to be possibly a prefrontal or lateral ethmoid. Gosline (1952) referred to this as an “antorbital strut” in *Echelus myrus* and considered it to be supportive for the maxilla. The senior author has seen this ossicle in microCT scans of several other species including two species of *Ilyophis*. The homology of this preorbital ossicle cannot be determined at the present time as its development and presence in other species of anguilliform fishes needs further study. There are 7–9 small lateral line ossicles in the dorsal branchial region posterior to the skull. These support the anterior portion of the lateralis nerve, where there are 4–5 small open pores in this region of the head.

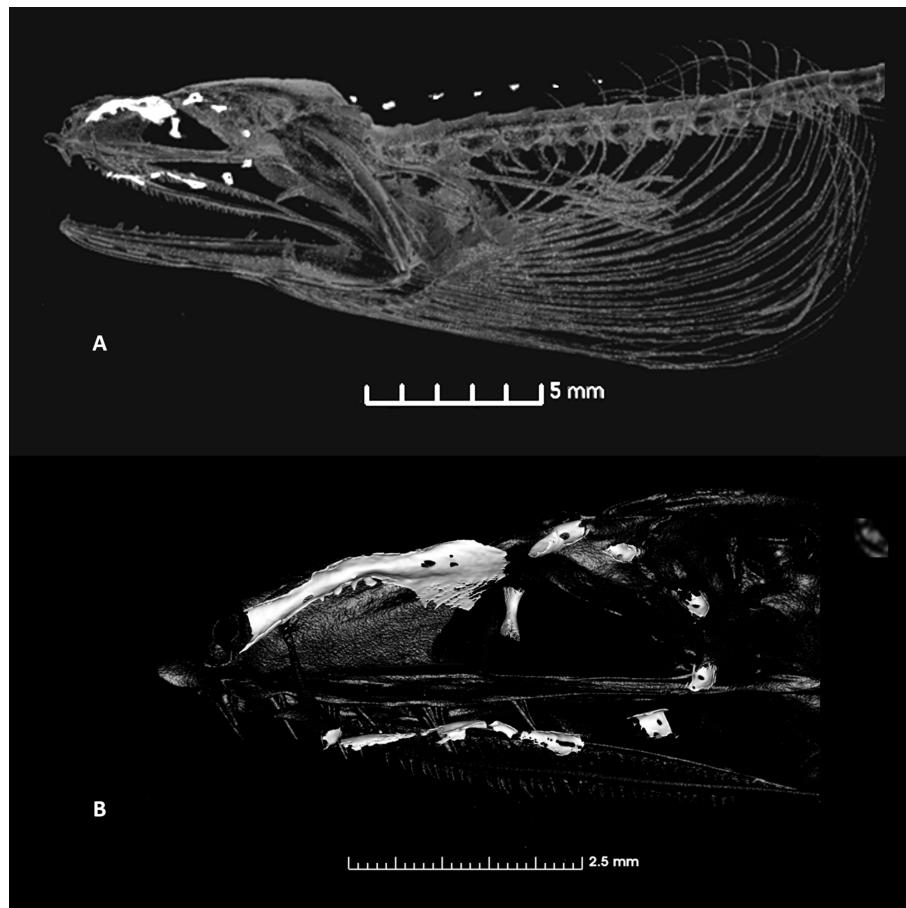


FIGURE 9. MicroCT scan of the anterior portion of *Branchenchelys megacephala*: A. Holotype BMNH 2016.8.25.788 showing cephalic and lateral line ossicles (white blotch-like areas). B. Paratype BMNH 2016.8.25.789, close-up showing morphology of cephalic ossicles.

Neurocranium (Fig. 10). The skull of *Branchenchelys megacephala* is lightly ossified and shows a generalized anguilliform pattern with the fused ethmovomer. The ethmovomer comprises the anterior 1/3 of the skull. There is a single frontal that covers nearly half of the dorsal surface of the skull. The remainder of the dorsal surface of the skull is composed of paired parietals, pterotics, epioccipitals, and sphenotics. In the holotype, there is no ossified supraoccipital visible although there is an open space that may represent a cartilaginous supraoccipital since cartilage does not show up in a standard microCT scan. The paratype does have a single, median supraoccipital in the same area. The ventral portion of the skull is composed of the fused ethmovomer, parasphenoid, prootics, exoccipitals, and basioccipital. In addition, the lateral portions of the pterosphenoids, pterotics, and sphenotics are visible in the ventral view. Despite the relatively small eye (4.0–5.6% HL), the orbit is relatively large and deep (Fig. 10B). The dorsal portion of the orbit is formed primarily by the frontal. The ethmovomer forms the anterior margin of the orbit, while the ventral and posterior margins are formed primarily by the parasphenoid and ventral processes of the frontal.

A unique character in the osteology of the neurocranium is found in the optic foramen at the back of the orbit. The optic foramen is relatively small and rimmed entirely by the frontal. In the paratype (Fig. 11 C–D), the ventral processes of the frontal extend down and around the foramen, and meet on the ventral midline, totally excluding the parasphenoid. In the holotype, these ventral processes form a complete ring around the foramen (Fig. 11A–B) and are fused on the ventral midline. In all other eels examined by the senior author, the rim of the orbital foramen is formed from the frontal along with the basisphenoid (if present) and the parasphenoid.

Suspensorium (Fig. 12). The left suspensorium with lower jaw and opercular series is shown in the figure. The hyomandibula is inclined posteriorly ca. 45 degrees. It articulates with the neurocranium anteriorly with a hemispherical “ball and socket” joint underneath the sphenotic and posteriorly in a groove along the ventral

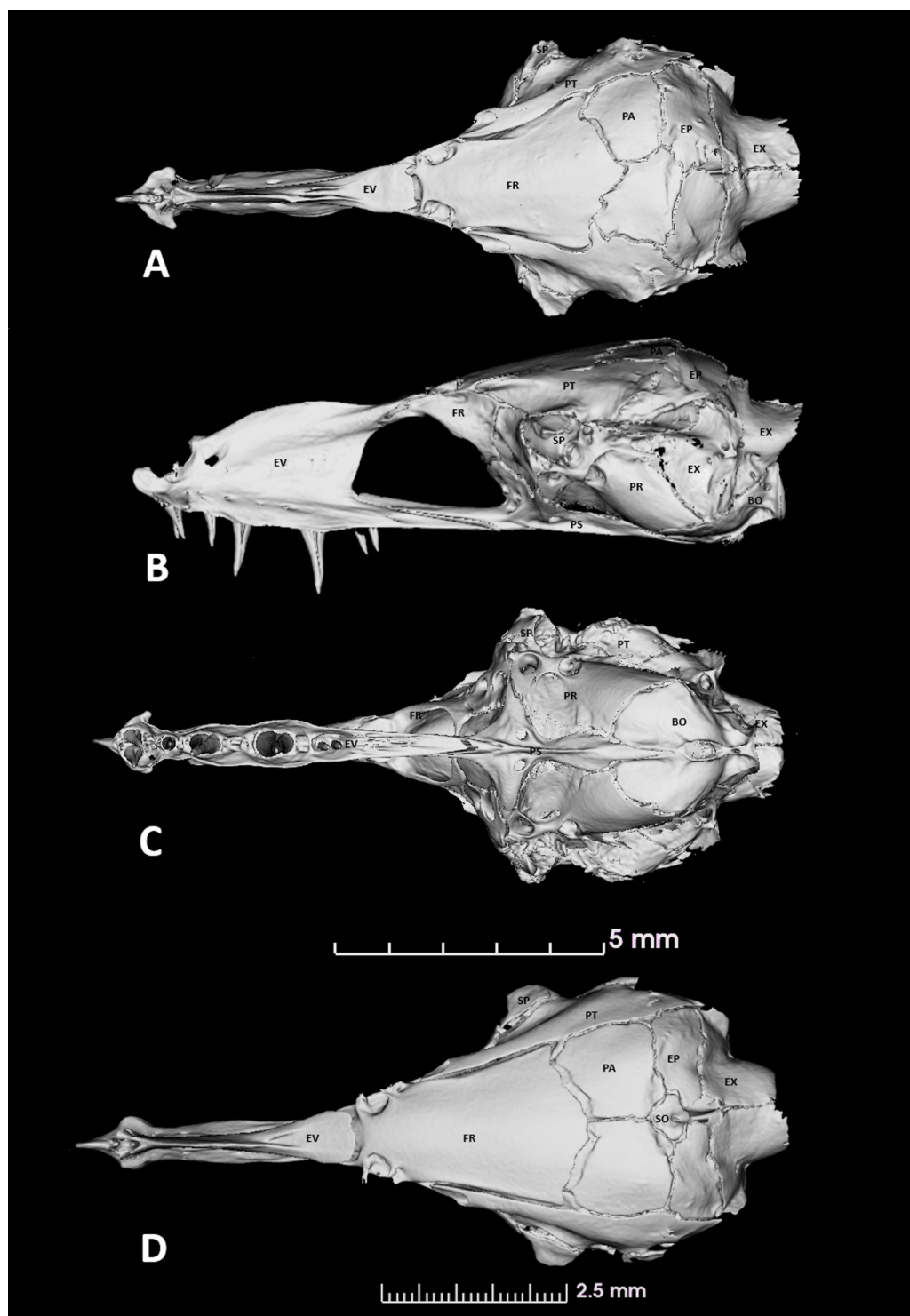


FIGURE 10. MicroCT scan of the neurocranium of *Branchenchelys megacephala*. A–C: holotype BMNH 2016.8.25.788. A. Dorsal view. B. Lateral view. C. Ventral view. D. paratype BMNH 2016.8.25.789, dorsal view. Abbreviations: BO, basioccipital; BS, basisphenoid; EP, epiotic; EV, Ethmovomerine; EX, exoccipital; FR, frontal; PA, parietal; PR, prootic; PS, parasphenoid; PT, pterotic; SO; supraoccipital; SP, sphenotic

surface of the pterotic. The hyomandibula and quadrate articulate in a complex interdigitated suture, with a long triangular process of the hyomandibula extending nearly to the articulation of the quadrate with the angulo-articulo-retroarticular. There is no ectopterygoid. The opercular series is complete with all four elements present, although greatly reduced in size and in ossification, especially along the margins. The opercle articulates with the

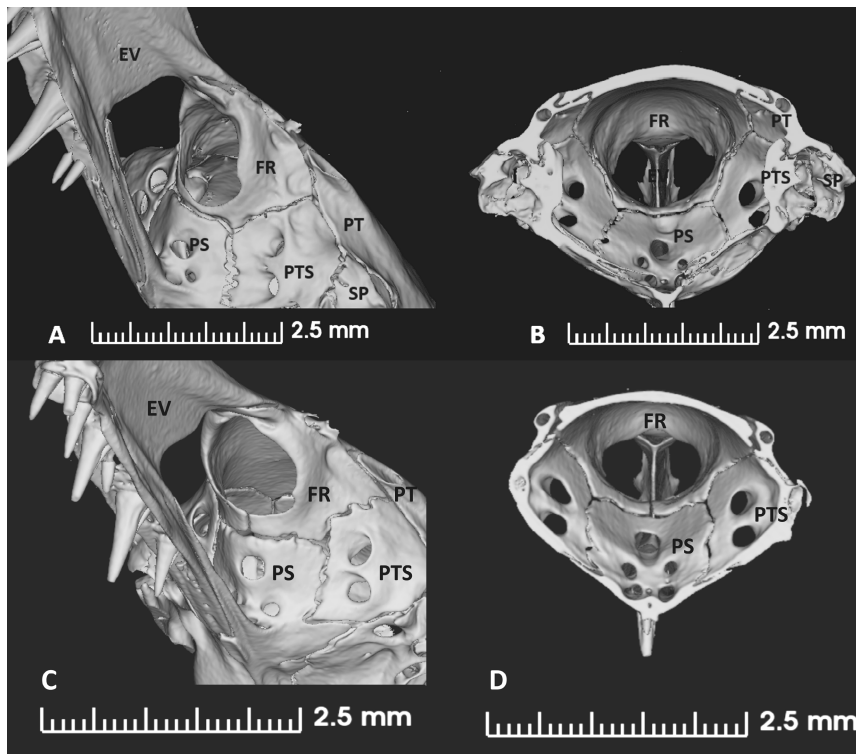


FIGURE 11. MicroCT scan of the optic foramen of *Branchenchelys megacephala*: A–B: holotype BMNH 2016.8.25.788. A. External view. B. Internal view. C–D: paratype BMNH 2016.8.25.789. C. External view. D. Internal view.

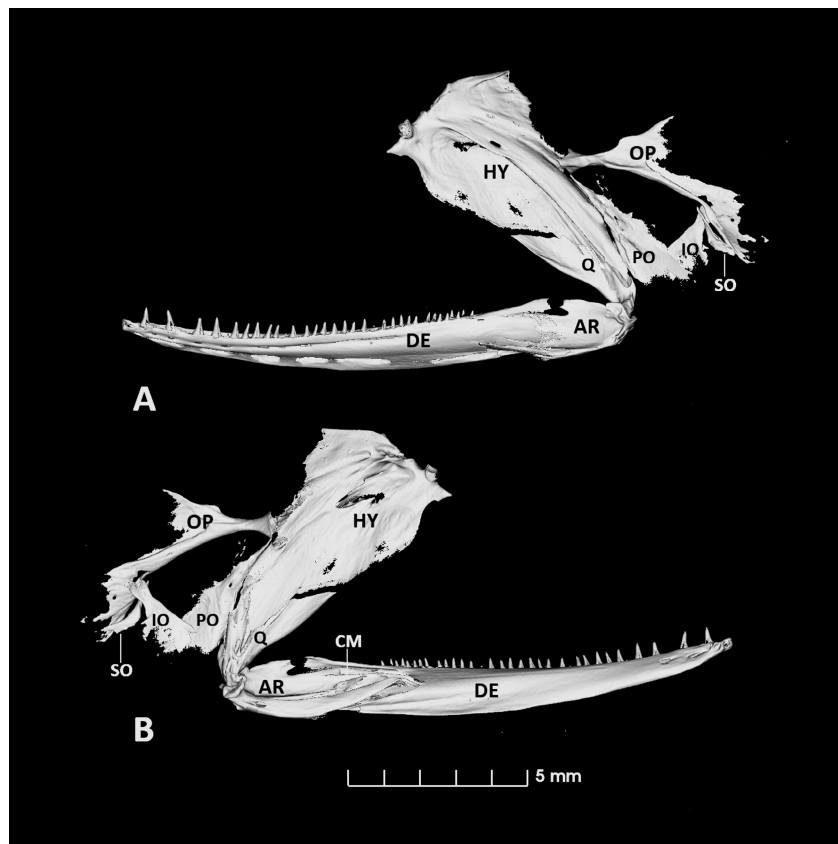


FIGURE 12. MicroCT scan of the suspensorium, opercular series and lower jaw of holotype of *Branchenchelys megacephala*: BMNH 2016.8.25.788. Lateral view. Abbreviations: AR, angulo-articulo-retroarticular; CM, coronomeckelian ossification; DE, dentary; HY, hyomandibular; IO, interopercle; OP, opercle; PO, preopercle; Q, quadrate; SO, subopercle.

hyomandibula through a bottle-neck articular condyle. The subopercle has an anterior arm that does not appear to articulate with any other bone of the opercular series. It is a very small bone lying just under the ventral margin of the opercle. The preopercle is an elongate triangular bone extending along the posterior margin of the hyomandibula from just below the articulation of the opercle with the hyomandibular down to just above the articulation between the hyomandibular and the quadrate. The interopercle is a triangular-shaped bone that is medial to the rest of the opercular series, extending from behind the preopercle to the lower margin of the opercle. Given the reduced size and ossification of the entire opercle series, it is unlikely that it provides much support for the branchial chamber.

Hyoid arch (Fig. 13). Basihyal and hypohyals are not present as ossified elements and no trace can be seen on the scans. The elements of the hyoid arch include anterior ceratohyals, posterior ceratohyals, and branchiostegal rays. The anterior ceratohyals are cylindrical tubes with a narrow splint of bone extending onto the dorsal surface of the posterior ceratohyals. The posterior ceratohyals are also cylindrical tubes but become laterally flattened and curve dorsally posteriorly. There are 23–25 branchiostegal rays; three to four originate on the anterior ceratohyal,

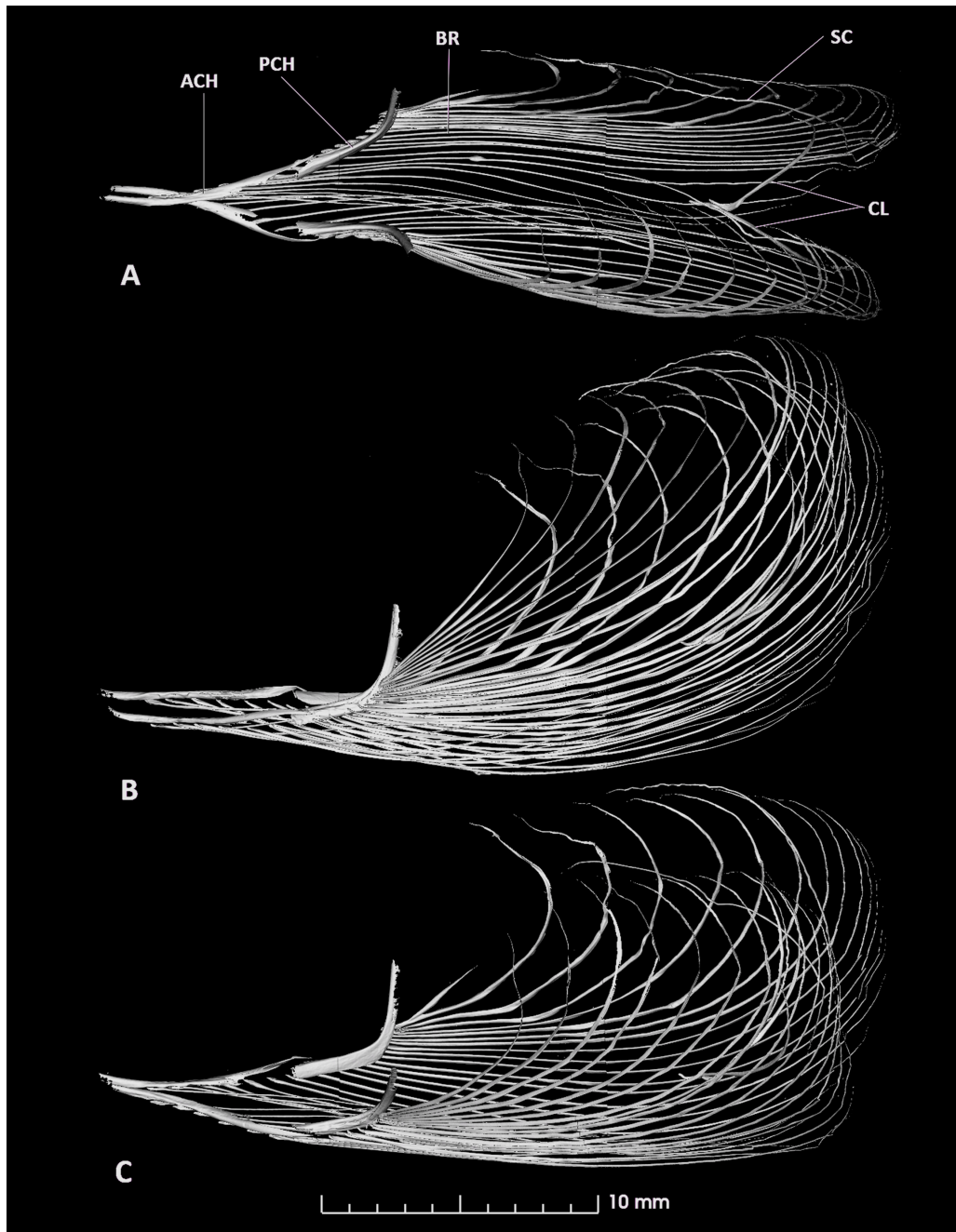


FIGURE 13. MicroCT scan of the hyoid arches of holotype of *Branchenchelys megacephala*: BMNH 2016.8.25.788. A. Dorsal view. B. Ventral view. C. Lateral view. D. Dorso-lateral view. Abbreviations: ACH, anterior ceratohyal; BH, basihyal; BR, branchiostegal rays; CL, cleithrum; HH, hypohyal; PCH, posterior ceratohyal; SC, supracleithrum.

three on the interspace between the anterior and posterior ceratohyals, and the rest on the posterior ceratohyal. An unusual aspect of the branchiostegals is the attachment of the posteriormost rays to the posterior ceratohyals. The last rays (5–7 in the holotype, 9 on each side of the paratype) have a single attachment point to the ceratohyal and then split distally into individual rays. There is no pectoral fin, but the remnants of the pectoral girdle include the cleithrum and supracleithrum which are found embedded within the branchiostegals near the posterior of the branchial chamber.

Branchial arches (Fig. 14). Basibranchials are not present as ossified elements and no trace can be seen on the scans. Ossified elements of the gill arches are the following: two pairs of hypobranchials, five pairs of ceratobranchials, four pairs of epibranchials, one pair of pharyngobranchials, and two pairs of pharyngobranchial toothplates. Both lower and upper pharyngobranchial toothplates are composed of two plates. The anterior lower pharyngobranchial toothplate is an elongate, slightly pointed oval and has a small number of small, conical teeth arranged in two irregular rows. The posterior upper pharyngobranchial toothplate is slightly triangular and has three rows of small, conical teeth. The anterior upper pharyngobranchial toothplate is an elongate triangular element with a small number of small, conical teeth at the posterior end. The posterior lower pharyngobranchial toothplate is a longer, irregularly triangular element covered with small, conical teeth arranged in five irregular rows.

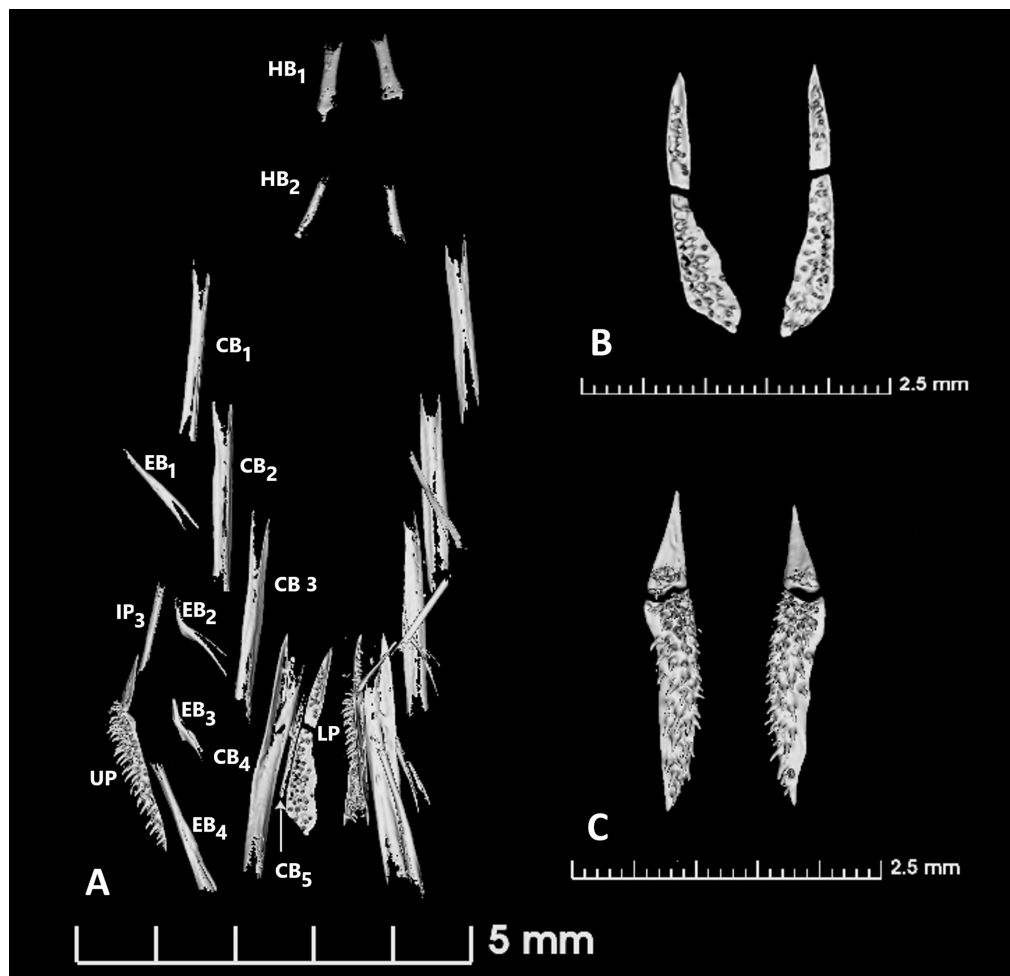


FIGURE 14. MicroCT scan of the branchial arches of paratype of *Branchenchelys megacephala*: BMNH 2016.8.25.789. A. Branchial arches in dorsal view, with upper elements of left branchial arch flipped to allow ventral view. B. Lower pharyngeal toothplates. C. Upper right pharyngeal toothplates. Abbreviations: CB, ceratobranchial; EB, epibranchial; HB, hypobranchial; IP, infrapharyngobranchial; LP, lower pharyngeal toothplate; UP, Upper pharyngeal toothplate.

Distribution. (Fig. 15). Western Indian Ocean: Arabian Sea; collected from two locations: off Oman and off Karnataka, southwest Indian coast. Given the large geographic range (ca. 1700 km) of the two localities, the species is probably more widely distributed within the Arabian Sea. However, since both localities are on the outer slopes of the continental shelf, the species may not be distributed within the deeper abyssal regions of the Arabian Sea.

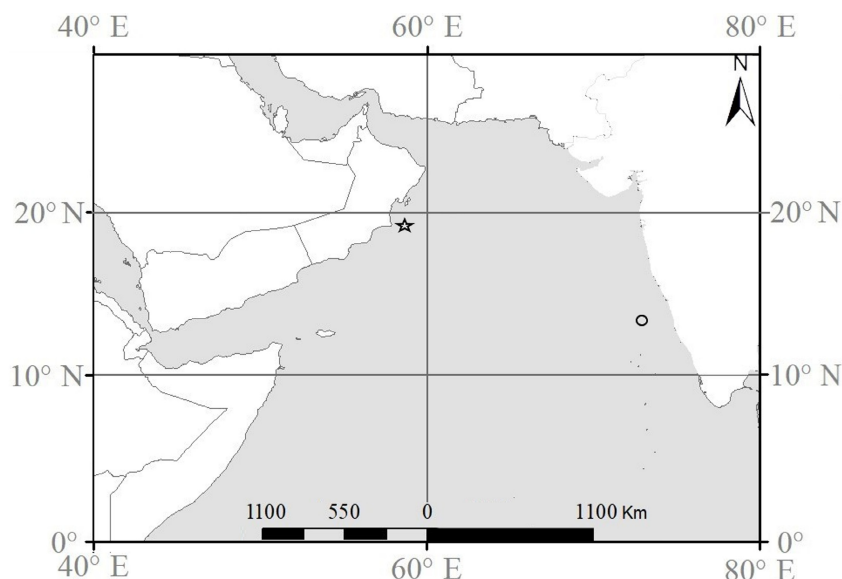


FIGURE 15. Distribution of *Branchenchelys megacephala* in the Arabian Sea, western Indian Ocean. Star is type locality, and circle is locality.

Etymology. The species name *megacephala* is derived from Greek μέγας meaning “big” and κεφάλι meaning “head” in reference to the large head of this species.

Remarks. The enlarged branchial chamber and greatly increased gill surface from the hypertrophied gill filaments are an adaptation to increase oxygen absorption in the oxygen-deficient waters of the Arabian Sea (Banse *et al.*, 2014). Gibbs and Hurwitz (1967) noted a large difference in the development of the gills between *Chauliodus pammelas* and *C. sloani* in the Indian Ocean. *C. pammelas*, which is distributed in the northern Arabian Sea, has much longer gill filaments with more numerous gill lamellae than *C. sloani*. Two other species of eels from the northern Indian Ocean also apparently have adaptations for the oxygen-deficient waters of the Arabian Sea and Bay of Bengal. *Sauromuraenesox vorax* Alcock, 1889 (Anguilliformes: Muraenesocidae) was described by Talwar (1977) as having a very large head (20.7–24.0% of total length) and relatively large gill openings (4.2–4.8% of total length). *Dysomma bucephalus* Alcock, 1889, another species in the subfamily Ilyophinae, was described by Karmovskaya (2023). She reported that this species also has a large head (23.9–24.8 of total length) and “gill openings greatly enlarged” (10.2–10.4 of head length, ca. 2.5 % of total length). Specimens of these two species were examined, and both species showed hypertrophied gill filaments, but not to the same degree as *Branchenchelys*.

Comparative material examined. *Dysomma bucephalus*: USNM 438265 (1, 191 mm TL); Indian Ocean, Bay of Bengal, off Myanmar, 16° 25' 53" N, 93° 56' 55" E, 277 m. USNM 438289 (2, 205–220 mm TL); Indian Ocean, Bay of Bengal, off Myanmar, 16° 47' 13" N, 94° 02' 09" E, 158 m. *Sauromuraenesox vorax*: USNM 410638 (2, 326–415 mm TL); Indian Ocean, Arabian Sea, S of Oman, 16° 23' 19" N, 54° 34' 52" E. USNM 438239 (2, 370–450 mm TL); Indian Ocean, Bay of Bengal, off Myanmar, 18° 14' 15" N, 93° 37' 52" E, 466 m. USNM 438255 (1, 470 mm TL); Indian Ocean, Bay of Bengal, off Myanmar, 16° 25' 53" N, 93° 56' 55" E, 277 m.

Acknowledgements

The first author would like to thank James MacLaine of The Natural History Museum, London, for bringing the BMNH specimens to his attention and making them available to him. He would also like to thank Matthew G. Girard and Leo MacLeod for their help with the microCT Scanner and 3D Slicer. The second author extends his gratitude to the Head, Centre for Marine Living Resources and Ecology (Ministry of Earth Sciences, Government of India), Kerala, for providing facilities and support. The authors are grateful to Shri. N. Saravanane for providing specimens collected during the exploratory surveys conducted by the FORV Sagar Sampada (Cruise No. 404). The authors also wish to thank Mr. Sanjay Kumar for providing the specimen collected from the Mangalore landing

centre. The authors also thank Vinicius C. Espíndola and Hauan-Ching Ho for their review and comments on the manuscript which greatly improved the final paper.

References

- Alcock, A. (1889) Natural History notes from H.M. Indian Marine Survey “Investigator,” Commander Alfred Carpenter, R.N., D.S.O., Commanding.—No. 13. On the bathybial fishes of the Bay of Bengal and neighboring waters, obtained during the seasons 1885–1889. *Annals and Magazine of Natural History*, Series 6, 4 (24), 450–461.
<https://doi.org/10.1080/00222938909460563>
- Banse, K., Naqvi, S.W.A., Narvekar, P.V., Postel, J.R. & Jayakumar, D.A. (2014) Oxygen minimum zone of the open Arabian Sea: variability of oxygen and nitrite from daily and decadal timescales. *Biogeosciences*, 11 (8), 2237–2261.
<https://doi.org/10.5194/bg-11-2237-2014>
- Böhlke, E.B. (1982) Vertebral formulae for type specimens of eels (Pisces: Anguilliformes). *Proceedings of the Academy of Natural Sciences, Philadelphia*, 134, 31–49.
- Böhlke, E.B. (1989) Methods and terminology. In: Böhlke, E.B. (Ed.), *Fishes of the Western North Atlantic. Memoir of the Sears Foundation for Marine Research*, 1 (Part 9), pp. 1–7.
- Chen, Y.-Y. & Mok, H.-K. (2001) A new synphobranchid eel, *Dysomma longirostrum* (Anguilliformes: Synphobranchidae), from the northeastern coast of Taiwan. *Zoological Studies*, 40 (2), 79–83.
- Chen, J.T.-F. & Weng, H.T.-C. (1967) A review of the apodal fishes of Taiwan. *Biological Bulletin Tunghai University Ichthyology Series*, No. 6 (Art. 32), 135–220.
- Fedorov, A., Beichel, R., Kalpathy-Cramer, J., Finet, J., Fillion-Robin, J.-C., Pujol, S., Bauer, C., Jennings, D., Fennessy, F., Sonka, M., Buatti, J., Aylward, S., Miller, J.V., Pieper, S. & Kikinis, R. (2012) 3D slicer as an image computing platform for the quantitative imaging network. *Magnetic Resonance Imaging*, 30, 1323–1341.
<https://doi.org/10.1016/j.mri.2012.05.001>
- Fricke, R., Eschmeyer, W.N. & van der Laan, R. (Eds.) (2025) Eschmeyer’s Catalog of Fishes: Genera, Species, References. Electronic version. Available from: <http://researcharchive.calacademy.org/research/ichthyology/catalog/fishcatmain.asp> (accessed 23 July 2025)
- Gibbs, R.H. Jr. & Hurwitz, B.A. (1967) Systematics and zoogeography of the stomiatoid fishes, *Chauliodus pammelas* and *C. sloani*, of the Indian Ocean. *Copeia*, 1967 (4), 798–805.
<https://doi.org/10.2307/1441889>
- Gosline, W.A. (1952) Notes on the systematic status of four eel families. *Pacific Science*, 42 (4), 130–135.
- Ho, H.-C., Smith, D.G. & Tighe, K.A. (2015) Review of the arrowtooth eel genera *Dysomma* and *Dysommia* in Taiwan, with the description of a new species (Anguilliformes: Synphobranchidae: Ilyophinae). *Zootaxa*, 4060 (1), 86–104.
<https://doi.org/10.11646/zootaxa.4060.1.12>
- Karmovskaya, E.S. (2023) First record of a rare eel *Dysomma bucephalus* (Synphobranchidae) in the Arabian Sea. *Journal of Ichthyology*, 63 (4), 616–626.
<https://doi.org/10.1134/S0032945223040094>
- Prokofiev, A.M. (2019) Three new eels of the genus *Dysomma* Alcock, 1889 from off Phuket Island, Thailand (Teleostei: Anguilliformes: Synphobranchidae). *Munis Entomology & Zoology*, 14 (2), 317–325.
- Robins, C.H. (1971) The comparative osteology of the synphobranchid eels of the Straits of Florida. *Proceedings of the Academy of Natural Sciences of Philadelphia*, 123 (7), 153–204.
- Robins, C.H. & Robins, C.R. (1970) The eel family Dysommidae (including the Dysommidae and Nettodaridae), its osteology and composition, including a new genus and species. *Proceedings of the Academy of Natural Sciences of Philadelphia*, 122 (6), 293–335.
- Robins, C.H. & Robins, C.R. (1976) New genera and species of dysommidae and synphobranchine eels (Synphobranchidae) with an analysis of the Dysommidae. *Proceedings of the Academy of Natural Sciences, Philadelphia*, 127 (18), 249–280.
- Robins, C.H. & Robins, C.R. (1989) Family Synphobranchidae. In: Böhlke, E.B. (Ed.), *Fishes of the Western North Atlantic. Memoir of the Sears Foundation for Marine Research*, 1 (Part 9), pp. 207–253.
<https://doi.org/10.2307/j.ctvbc0dm.12>
- Saruwatari, T., López, J.A. & Pietsch, T.W. (1997) Cyanine Blue: A versatile and harmless stain for specimen observation. *Copeia*, 1997 (4), 840–841.
<https://doi.org/10.2307/1447302>
- Talwar, P.K. (1977) Identity of the deep-sea eel, *Sauromuraenesox vorax* Alcock (Anguilliformes: Muraenesocidae). *Proceedings of the Zoological Society of Calcutta*, 30, 51–55.